Electronic Supplementary Material (ESI) for Dalton Transactions.

Electronic Supplementary Information (ESI)

Three sra topological lanthanide-organic frameworks built from 2,2'-dimethoxy-4,4'-biphenyldicarboxylic acid

Xin Wang,[a] Jie Zhao,[a] Yan Zhao,[c] Heng Xu,[a] Xuan Shen,[a] Dun-Ru Zhu*,[a,d] and Su Jing*,[b]

[a] *College of Chemistry and Chemical Engineering, State Key Laboratory of Materials-oriented Chemical Engineering,* [b] *College of Science, Nanjing Tech University, Nanjing 210009, P. R. China,* [c] *School of Environmental Science and Engineering, North China Electric Power University, Baoding, 071003, Hebei, P. R. China,* [d] *State Key Laboratory of Coordination Chemistry, Nanjing University, Nanjing 210093, P. R. China*

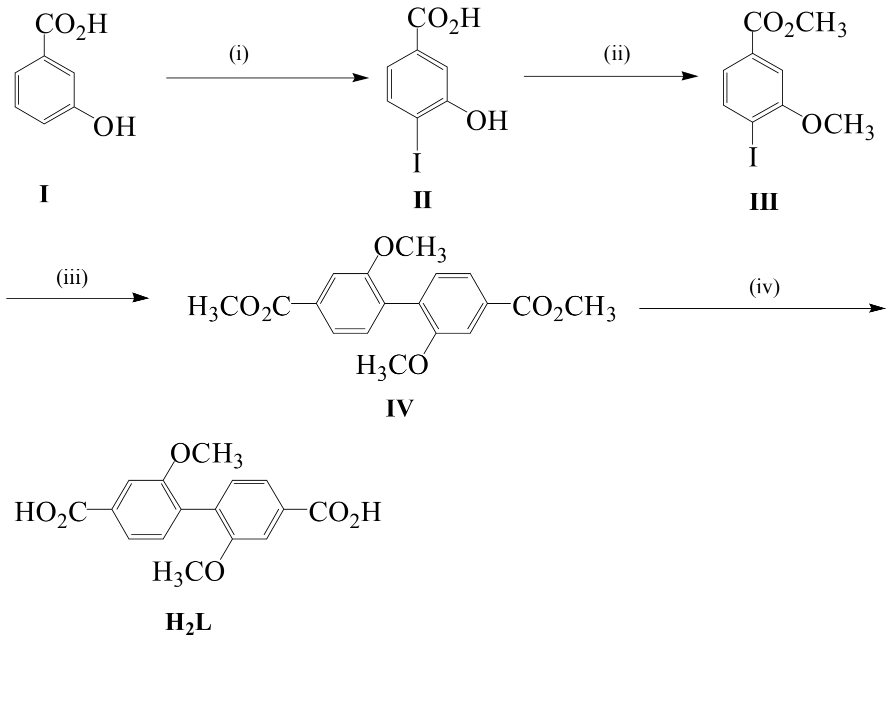

Scheme S1. The synthetic route of 2,2'-dimethoxy-biphenyl-4,4'-dicarboxylic acid (H_2L): (i) concentrated aqueous ammonia, KI, I_2, H_2O, (ii) dimethyl sulfate, K_2CO_3, acetone, (iii) activated copper powder, 210-220 °C, (iv) a) KOH, methanol, reflux, 1h; b) HCl.

The commercially available *m*-hydroxybenzoic acid (**I**) reacting with potassium iodide and iodine in concentrated aqueous ammonia solution gave 3-hydroxy-4-iodobenzoic acid (**II**) in a yield of 62%.[1] Brief treatment of **II** with $(CH_3)_2SO_4$ produced methyl 4-iodo-3-methoxybenzoate (**III**) in a yield of 84%.[2] By use of the Ullmann reaction **III** was converted into dimethyl 2,2'-dimethoxy-4,4'-biphenyldicarboxylate (**IV**) in a yield of 74% under argon atmosphere.[3]

Table S1 Selected bond lengths (Å) for LOFs **1–3**

1		**2**		**3**	
Eu1-O2^{i}	2.314(4)	Gd1-O2^{i}	2.309(3)	Dy1-O2^{v}	2.276(4)
Eu1-O1	2.338(3)	Gd1-O1	2.328(3)	Dy1-O1	2.297(3)
Eu1-O4^{ii}	2.340(3)	Gd1-O4^{ii}	2.334(3)	Dy1-O4^{vi}	2.304(4)
Eu1-O3^{iii}	2.355(3)	Gd1-O3^{iii}	2.341(3)	Dy1-O3^{vii}	2.306(3)
Eu1-O7	2.389(4)	Gd1-O7	2.381(3)	Dy1-O7	2.362(4)
Eu1-O8^{i}	2.434(4)	Gd1-O8^{i}	2.430(3)	Dy1-O8^{v}	2.410(4)
Eu1-O9	2.528(4)	Gd1-O9	2.512(3)	Dy1-O9	2.491(4)
Eu1-O8	2.579(4)	Gd1-O8	2.568(3)	Dy1-O8	2.548(4)
Eu1-Eu1^{iv}	4.448(4)	Gd1-Gd1^{iv}	4.445(3)	Dy1-Dy1^{viii}	4.414(4)

Symmetry codes: i) -*x*, 3-*y*, *z*-1/2; ii) 1/2-*x*, *y*-1/2, *z*-1/2; iii) *x*-1/2, 7/2-*y*, *z*; iv) -*x*, 3-*y*, *z*+1/2; v) 2-*x*, -*y*-1, *z*+1/2; vi) 3/2-*x*, *y*+1/2, *z*+1/2; vii) *x*+1/2, -*y*-3/2, *z*; viii) 2-*x*, -*y*-1, *z*-1/2.

Table S2 Selected bond angles (°) for LOFs **1–3**

1					
O1–Eu1–O2^{i}	155.13(14)	O3^{iii}–Eu1–O7	143.40(14)	O3^{iii}–Eu1–O9	79.93(13)
O2^{i}–Eu1–O4^{ii}	81.78 (13)	O2^{i}–Eu1–O8^{i}	80.77(14)	O7–Eu1–O9	71.80(14)
O1–Eu1–O4^{ii}	82.24(12)	O1–Eu1–O8^{i}	76.47(12)	O8^{i}–Eu1–O9	146.93(12)
O2^{i}–Eu1–O3^{iii}	80.69(13)	O4^{ii}–Eu1–O8^{i}	73.46(12)	O2^{i}–Eu1–O8	121.43(13)
O1–Eu1–O3^{iii}	102.71(13)	O3^{iii}–Eu1–O8^{i}	75. 04(11)	O1–Eu1–O8	82.49(12)
O4^{ii}–Eu1–O3^{iii}	145.93(13)	O7–Eu1–O8^{i}	139.11(13)	O4^{ii}–Eu1–O8	141.47(12)
O2^{i}–Eu1–O7	112.17(14)	O2^{i}–Eu1–O9	74.07(14)	O7–Eu1–O8	72.02(13)

O1–Eu1–O7	79.97(15)	O1–Eu1–O9	130.78(14)	O8^{i}–Eu1–O8	135.68(7)
O4^{ii}–Eu1–O7	70.59(13)	O4^{ii}–Eu1–O9	122.45(13)	O9–Eu1–O8	50.99(12)
O3^{iii}–Eu1–O8	72.20(11)	Eu1^{iv}–O8–Eu1	125.05(14)		
		2			
O2^{i}–Gd1–O1	155.36(12)	O2^{i}–Gd1–O8^{i}	80.79(12)	O7–Gd1–O9	71.88(13)
O2^{i}–Gd1–O4^{ii}	81.94(11)	O1–Gd1–O8^{i}	76.53(11)	O8^{i}–Gd1–O9	146.49(11)
O1–Gd1–O4^{ii}	82.52(11)	O4^{ii}–Gd1–O8^{i}	73.54(11)	O2^{i}–Gd1–O8	121.41(11)
O2^{i}–Gd1–O3^{iii}	81.19(12)	O3^{iii}–Gd1–O8^{i}	74.75(10)	O1–Gd1–O8	82.24(10)
O1–Gd1–O3^{iii}	101.75(11)	O7–Gd1–O8^{i}	139.20(12)	O4^{ii}–Gd1–O8	141.02(10)
O4^{ii}–Gd1–O3^{iii}	146.00(11)	O2^{i}–Gd1–O9	73.53(12)	O3^{iii}–Gd1–O8	72.50(10)
O2^{i}–Gd1–O7	111.57(13)	O1–Gd1–O9	131.10(12)	O7–Gd1–O8	71.97(11)
O1–Gd1–O7	80.68(13)	O4^{ii}–Gd1–O9	122.34(11)	O8^{i}–Gd1–O8	136.01(6)
O4^{ii}–Gd1–O7	70.26(11)	O3^{iii}–Gd1–O9	80.27(11)	O9–Gd1–O8	51.31(10)
O3^{iii}–Gd1–O7	143.68(12)	Gd1^{iv}–O8–Gd1	125.57(11)		
		3			
O2^{iv}–Dy1–O1	155.66(15)	O2^{iv}–Dy1–O8^{iv}	80.75(15)	O7–Dy1–O9	71.45(15)
O2^{iv}–Dy1–O4^{v}	82.20(14)	O1–Dy1–O8^{iv}	77.09(13)	O8^{iv}–Dy1–O9	146.50(13)
O1–Dy1–O4^{v}	82.08(13)	O4^{v}–Dy1–O8^{iv}	73.80(13)	O2^{iv}–Dy1–O8	121.95(14)
O2^{v}–Dy1–O3^{vii}	81.11(14)	O3^{vii}–Dy1–O8^{v}	74.69(12)	O1–Dy1–O8	81.54(12)
O1–Dy1–O3^{vii}	102.36(13)	O7–Dy1–O8^{v}	139.60(14)	O4^{vi}–Dy1–O8	140.55(13)
O4^{vi}–Dy1–O3^{vii}	146.25(14)	O2^{v}–Dy1–O9	73.83(16)	O3^{vii}–Dy1–O8	72.62(12)
O2^{v}–Dy1–O7	111.01(15)	O1–Dy1–O9	130.48(15)	O7–Dy1–O8	72.02(13)
O1–Dy1–O7	80.65(15)	O4^{vi}–Dy1–O9	122.59(14)	O8^{v}–Dy1–O8	135.68(8)
O4^{vi}–Dy1–O7	70.04(14)	O3^{vii}–Dy1–O9	80.08(14)	O9–Dy1–O8	51.50(13)
O3^{vii}–Dy1–O7	143.63(15)	Dy1^{viii}–O8–Dy1	125.81(14)		

Symmetry codes: i) -*x*, 3-*y*, *z*-1/2; ii) 1/2-*x*, *y*-1/2, *z*-1/2; iii) *x*-1/2, 7/2-*y*, *z*; iv) -*x*, 3-*y*, *z*+1/2; v) 2-*x*, -*y*-1, *z*+1/2; vi) 3/2-*x*, *y*+1/2, *z*+1/2; vii) *x*+1/2, -*y*-3/2, *z*; viii) 2-*x*, -*y*-1, *z*-1/2.

Table S3 Hydrogen-bonding geometry (Å, °) for LOF **2**

D–H···A	d(D–H)	d(H···A)	d(D···A)	∠D–H···A
C18–H18B···O4^{ix}	0.96	2.49	3.440(8)	169
C18–H18A···O7	0.96	2.29	2.718(4)	106

Symmetry code: ix) -*x*-1/2, *y*+5/2, *z*+1/2.

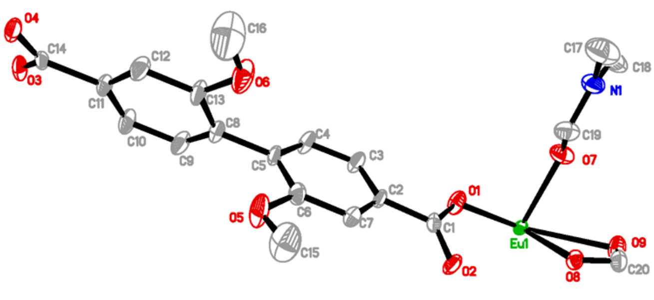

Fig. S1 OPTER drawing (at 50% probability) of the asymmetric unit for LOF **1** (Hydrogen atoms are omitted for clarity).

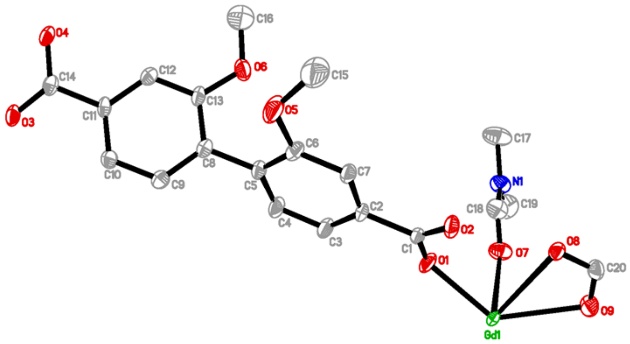

Fig. S2 ORTEP drawing (at 50% probability) of the asymmetric unit for LOF **2** (Hydrogen atoms are omitted for clarity).

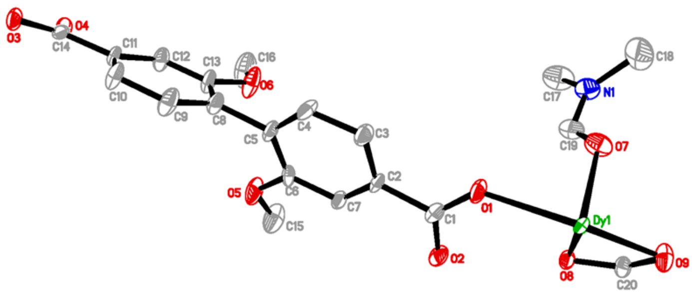

Fig. S3 ORTEP drawing (at 50% probability) of the asymmetric unit for LOF **3** (Hydrogen atoms are omitted for clarity).

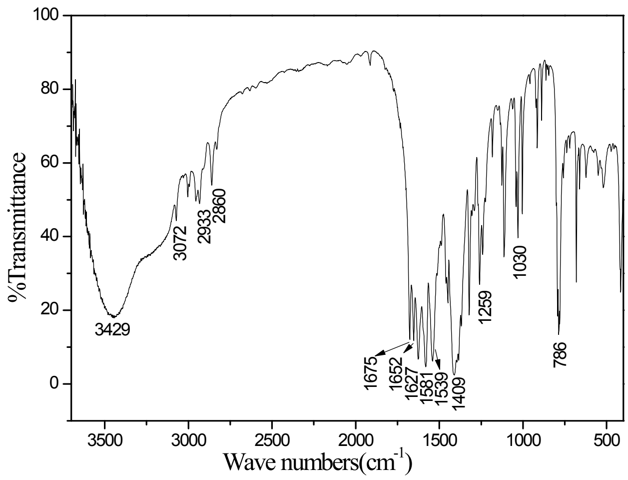

Fig. S4 The IR spectra of LOF **1**.

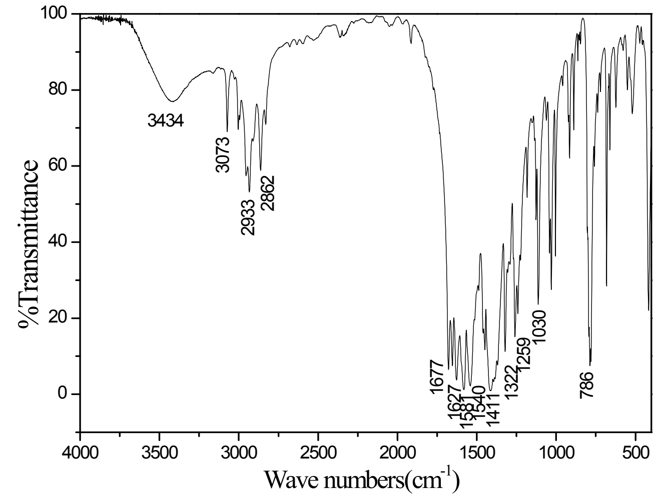

Fig. S5 The IR spectra of LOF **2**.

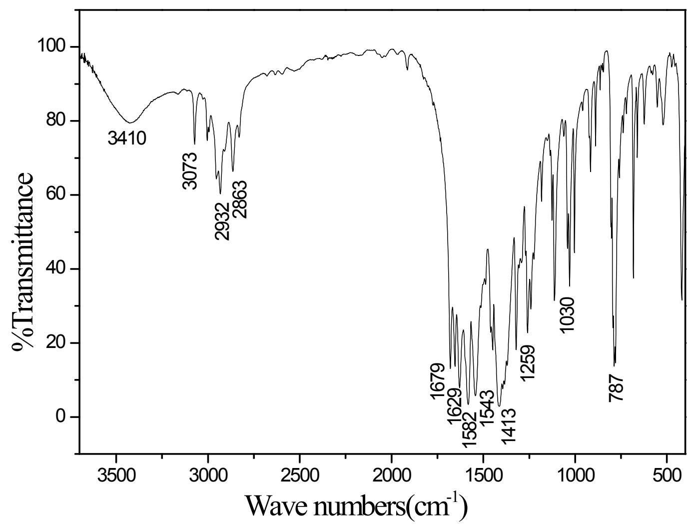

Fig. S6 The IR spectra of LOF **3**.

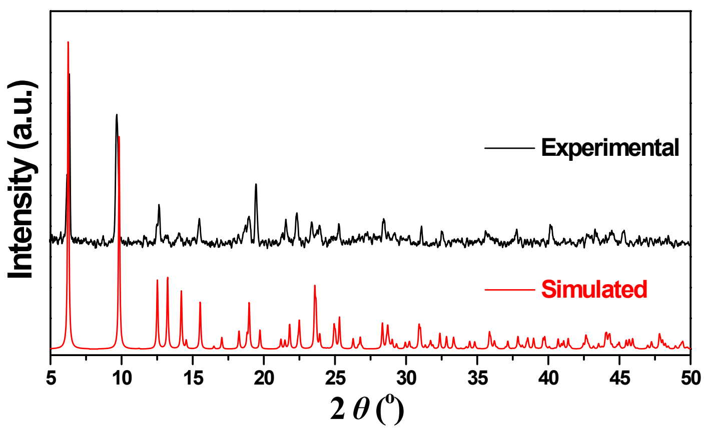

Fig. S7 Experimental and simulated powder X-ray diffraction patterns of LOF **1**.

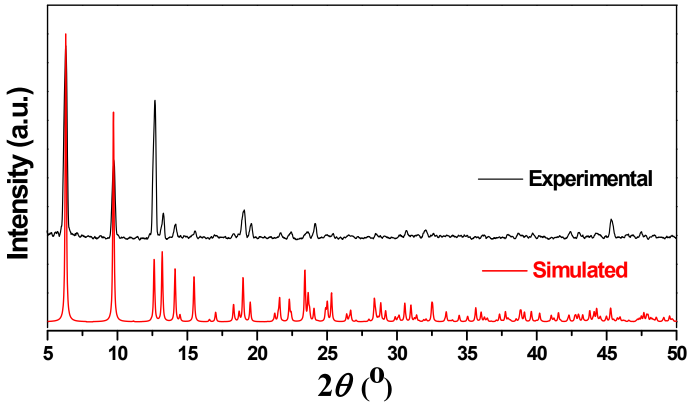

Fig. S8 Experimental and simulated powder X-ray diffraction patterns of LOF **2**.

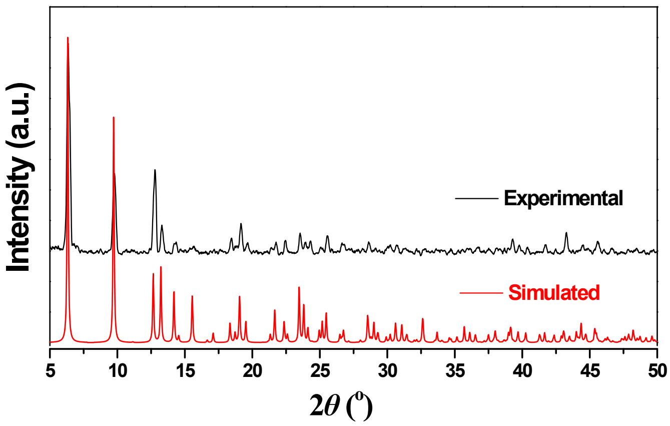

Fig. S9 Experimental and simulated powder X-ray diffraction patterns of LOF **3**.

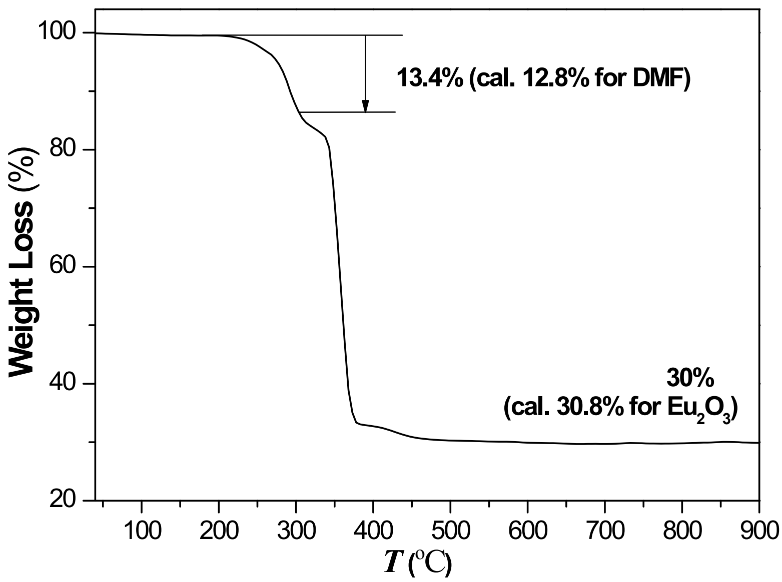

Fig. S10 TGA curve for LOF **1**.

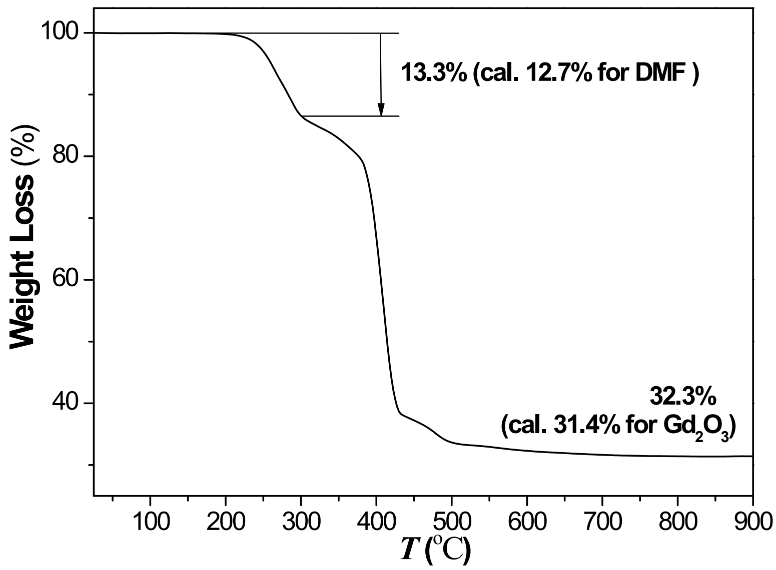

Fig. S11 TGA curve for LOF **2**.

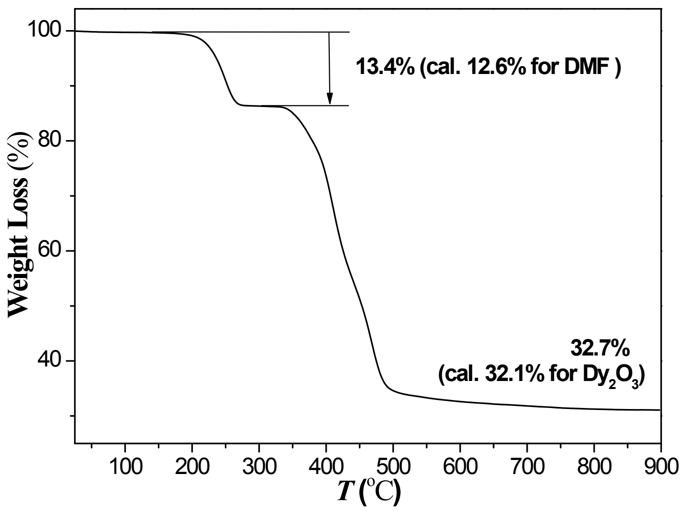

Fig. S12 TGA curve for LOF **3**.

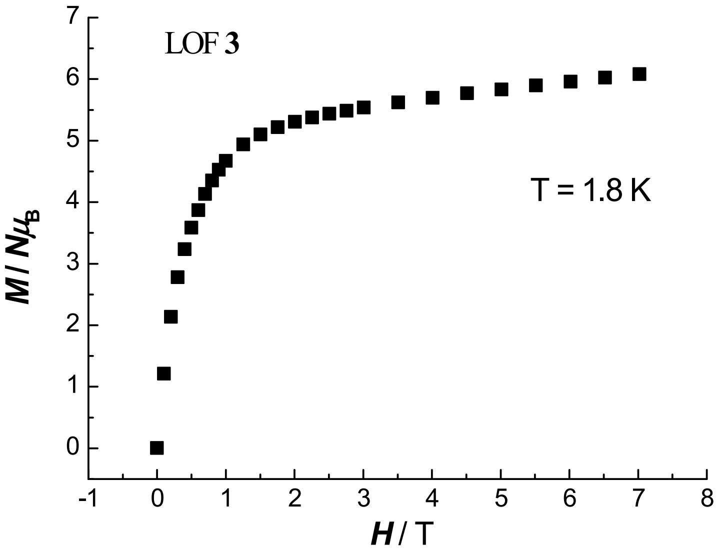

Fig. S13 M-H plot for **3** at 1.8 K.

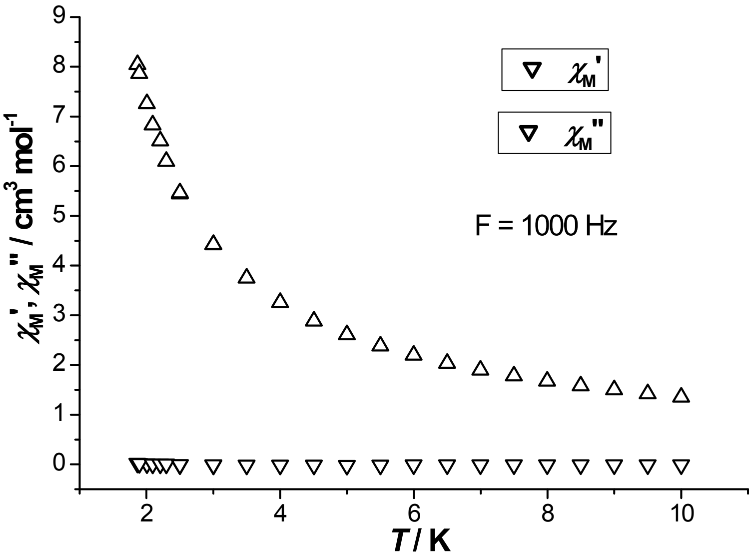

Fig. S14 Variable-temperature AC magnetic susceptibilities of **3** in an ac field of 5 Oe with an oscillating frequency of 1000 Hz.

References

1 (a) H. R. Frank, P. E. Fanta and D. S. Tarbell, *J. Am. Chem. Soc.*, 1948, **70**, 2314; (b) K. Sagi, T. Nakagawa, M. Yamanashi, S. Makino, M. Takahashi, M. Takayanagi, K. Takenaka, N. Suzuki, S. Oono, N. Kataoka, K. Ishikawa, S. Shima, Y. Fukuda, T. Kayahara, S. Takehana, Y. Shima, K. Tashiro, H. Yamamoto, R. Yoshimoto, S. Iwata, T. Tsuji, K. Sakurai and M. Shoji, *J. Med. Chem.*, 2003, **46**, 1845; (c) R. J. Pilling and D. A.

Whiting, *J. Chem. Soc., Perkin Trans. 1*, 1999, 2077; (d) P. Brenans and C. Prost, *Compt. Rend.*, 1924, **178**, 1285.

2 (a) A. Speicher, J. Kolz and R. P. Sambanje, *Synthesis*, 2002, 2503; (b) G. Dunet and P. Knochel, *Synlett*, 2007, 1383.

3 (a) T. R. Govindachari, N. Viswanathan, K. R. Ravindranath and B. Anjaneyulu, *Indian J. Chem.*, 1973, **11**, 1081; (b) M. A. Rizzacasa and M. V. Sargent, *Aust. J. Chem.*, 1988, **41**, 1087.